Design of a module for a 10 {MJ} toroidal {YBCO} Superconducting Magnetic Energy Storage

Design of a module for a 10 MJ toroidal YBCO Superconducting Magnetic Energy Storage

Simone Sparacio, Andrea Napolitano, Laura Savoldi, *Member, IEEE,* Sofia Viarengo and Francesco Laviano

***Abstract*— In this work, we presented the design of a module of a 10 MW toroidal SMES, tailored for a charge/discharge time of 1 s aimed at compensating the intermittency of a solar photovoltaic system. The design is performed through an approach based on the functional analysis: first, the functions that must be satisfied by the SMES are identified, together with constraints such as the performance of commercial YBCO tapes. Then, the pre-conceptual design of, among the different components, the winding pack and the cryostat is performed, to cope with the constraints and comply with the assigned functions. Finally, the design is verified through a detailed numerical analysis, checking that the requested function is in fact satisfied. The design leads to a multi-layer coil with radius ~ 0.45 m, wound using a stack of 7 commercial 12 mm-width tapes with 52 layers in parallel, each with 26 turns. The total inductance is ~2 H and a maximum self-field below 4 T. Nine modules are needed for the entire SMES, which is designed to operate at 50 K.**

***Index Terms*—Energy storage, SMES, HTS coils, renewable energy source.**

I. Introduction

THE progressively increasing penetration of electricity from solar photovoltaic (PV) plants, needed for a successful deployment of renewable energy sources, strongly depends on the economic cost of system integration, that should also mitigate the intermittency of PV electricity. Among the different available energy storage systems that could be applied to compensate the fluctuating PV power, Superconductive Magnetic Energy Storage (SMES) are attractive because of their high deliverable power and efficiency, and their virtually infinite number of charge-discharge cycles without degradation. Hence, many studies and developments of SMES have been carried out. A macroscopic classification about research on SMES systems can be split into three main fields: circuit topology and control techniques of the Power Conversion System (PCS), feasible application and control methods, and design and optimization of the superconducting magnets [1]. The cooling and the protection system are also an integral part of the SMES. A quite complete overview of SMES application in power and energy system has been reported in [2]. Depending on the application and the design criteria, three main PCS topologies have been deeply investigated: thyristor based, Voltage Source Converter (VSC) based, and Current Source Converter (CSC) based SMES. Regarding the coil design, both the solenoidal and the toroidal configuration are studied and optimized, showing their own pros and cons [3]–[8]. Here, we present the design of a module for a 10 MW toroidal YBCO SMES, with a charge/discharge time of 1 s, including the superconducting coil, the power feeding system, and the cryogenic cooling. The adopted constraints (i.e., maximum external diameter, working temperature) have been chosen such that the system can efficiently operate (trade-off between thermo-magnetic properties and dimensions) within a MW-range PV plant. The design is based on the functional analysis approach: the functions that must be satisfied by the SMES are first identified, then the different components are defined and designed, capable to comply with the assigned function, and the set of operating constraints. The conceptual design of the cryostat is also presented, focusing on the thermal insulation and the cryocooler.

II. Functional analysis of the SMES

The design of the SMES module has been performed with a functional analysis approach, translating the system-level requirements into detailed functional and performance requirements for the sub-components. The maximum value for the module radius of 0.5 m (considering ~ 1 m^3 as handy dimension for a medium size PV plant) and a maximum magnetic self-field of 4 T have been set as design constraints. The function tree is presented on Figure 1. The functions are classified into process functions, if they deal directly with the operation of the SMES at the nominal set of parameters, and functions to protect the investment, dealing with the components that should guarantee that any off-normal condition is detected and possibly avoided.

A. Process functions

The two main process functions of a SMES system are the absorption and the release of electric power within fraction of cycle and the storage of magnetic energy for long time and with high efficiency. Below these ‘top level’ functions, a series of ‘lower-level’ ones can be identified on a general ground and on a more detailed perspective, depending on the specific application. For instance, concerning the design criteria of the PCS, it must be able to supply uninterruptible power during short time interruption of the grid supply, to compensate the reactive power

Submitted for review on September 6, 2021.

L. Savoldi and S. Viarengo are with the MAHTEP Group, Dipartimento Energia “Galileo Ferraris”, Politecnico di Torino, Torino 10129, Italy (e-mail: laura.savoldi@polito.it, sofia.viarengo@polito.it).

S. Sparacio, F. Laviano and A Napolitano are with the SM-MESH Group, Dipartimento Scienza Applicata e Tecnologia, Politenico di Torino, Torino 10129, Italy (e-mail: simone.sparacio@polito.it, francesco.laviano@polito.it, andrea.napolitano@polito.it).

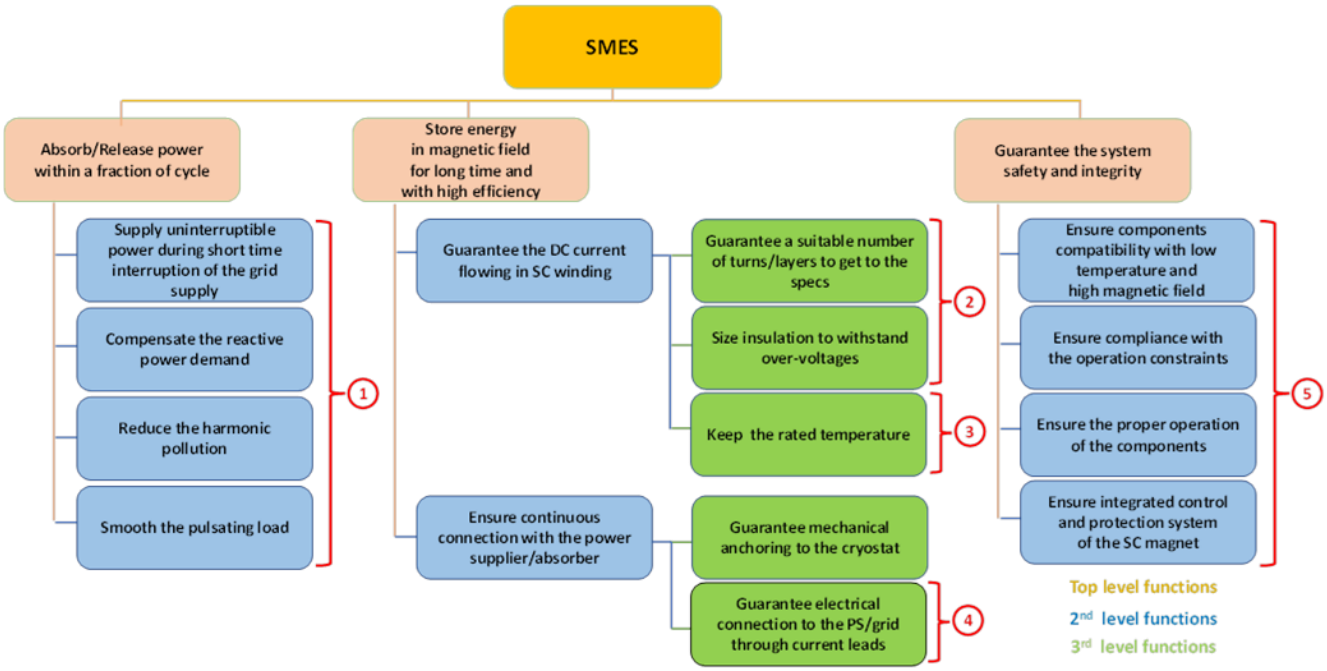

Figure 1. SMES function tree: 1 = Power Conditioning System; 2 = Winding Pack; 3 = Dewar; 4 = Power feeding system; 5 = Control and protection system.

demand, to smooth the pulsating load, and to reduce the harmonic pollution of the grid. Moreover, one must guarantee the continuous current flow to be within superconducting windings and ensure the continuous connection with the power supplier/absorber. The latter is the core of the present work, and the related sub-systems are designed in such a way that each constitutive component full-fills its own independent function, as shown at the third level of the functional analysis (green boxes of Figure 1), and its own constraints.

B. *Functions to protect the investment*

The safety and the integrity of the whole system should be guaranteed by proper functions to protect the investments. They integrate the control and protection system requirements to detect and possibly avoid any abnormal conditions, protecting the mildest components, and ensuring the required work compliance.

III. SUB-SYSTEMS AND COMPONENTS IDENTIFICATION

The SMES must be composed by a number of elements able to satisfy each of the independent function identified in the previous functional analysis:

1. *Power conditioning system (PCS):* for regulating the electricity exchange between the SMES and the grid – it converts the current from AC to DC, and vice versa, and charges and discharges the coil.
2. *Winding Pack (WP):* for storing the magnetic energy without joule losses (excluding those in AC mode operation).
3. *Dewar:* that includes: a cryostat, which walls must offer excellent thermal insulation in order to minimize heat flow into the cryogenic region, A cryogenic auxiliary system which maintains the coil temperature below the critical temperature of the superconductor.
4. *Power Feeding System:* to guarantee electrical connections to the power supplier (PS)/absorber and the grid.
5. *Control and protection system:* for establishing a link between power demands from the grid and power flow to or from the SMES coil. It receives dispatch signals from the power grid and status information from the SMES coil, the refrigerator, and from other equipment. It also detects and protects the system from any abnormal condition that may cause safety hazard to personnel or damage the magnet.

IV. WINDING PACK DESIGN

The design of a winding pack must guarantee a suitable number of turns/layers to get to the required specifications, a proper sized insulation to withstand normal and off-normal over-voltages and a continuum electrical connection to the PS/grid by means of current leads. The ampere-turn design is based on a stack of 7 commercial 12 mm-width 2G YBCO tapes (0.1 mm-thick each), with a nominal current of more than 300 A at 77 K, so that conservatively a total effective current of 1 kA at 50 K can be retained for the stack. The choice of the 12 mm-width results from a gradient search optimization process which brought to the highest inductance with the lowest stack length compared to the other available products (4 mm, 6 mm) of the same factory. The main specifications of the adopted tape, including the specific Ic(B) property, are taken from [9]. For the winding pack of a single module, the optimized design points to a multi-layer coil with radius ~ 0.45 m, wound using 52 layers in parallel, each with 26 turns, with a total inductance of ~2 H and a maximum self-field below 4 T. Nine modules are needed for the entire SMES. Such design is checked and validated by a detailed 2D axisymmetric electro-magnetic model, purposely developed in COMSOL Multiphysics® [10].

A. Methodology

One of the main goals when designing a SMES is to maximize the stored energy while minimizing the volume of the HTS coil (i.e., minimizing the required amount of HTS tape). Eq. (1) gives the basis for superconducting magnetic energy storage.

$$E = \frac{1}{2} L I^2 \quad (1)$$

Once the operating current is set, the inductance puts the limits on the system performance. A gradient search algorithm is performed to maximize the self-inductance of the module with the lowest stack length, which is one of the most limiting factors in terms of cost. The objective function has been optimized respecting the following functional constraints: outer radius lower than 0.5m, inner radius higher than the minimum bending radius of the considered tape and a maximum magnetic field lower than 4 T. The Wheeler's formulas, Eq. (2), for a rectangular cross-section multi-layer air core solenoid, is adopted in the model [11].

$$L = \frac{0.8(r^2 N_{turn}^2 N_{layer}^2)}{6r + 9b + 10c} \quad (2)$$

Here, *r* is average radius of windings, *b* is height and *c* is the thickness of the coil. The results of the optimization analysis are reported in Table 1.

Around each stack 0.1 mm polyimide film is then used for electrical insulation. The latter has been designed to withstand to a puncture breakdown of about 30 kV. The choice has been done considering 10 times off-normal over-voltage with respect the one that occurs during normal charging and discharging phase (~ 3 kV considering half-energy charge/discharge, with a cut-off frequency of 2 Hz).

The entire module is then covered by 0.3 mm polyimide film for mechanical stability and magnet-to-cryostat/ground insulation. A 3 mm-thick Aluminum 6061-T6 is adopted as gravity support and for withstanding the Lorentz forces. Figure 2 summarizes the basic design geometry of the SMES module.

B. Design validation

To validate the design a 2D axisymmetric FEM model has been built on COMSOL Multiphysics®. The AC/DC module is used to describe the stationary electro-magnetic behavior of the present coil. The magnetic field within all domains but the SC stacks is described by the Ampere law. The stacks are modelled as standard conductors (linear constitutive relation with 'infinite' electrical conductivity) transporting a current of 1050 A. Because of the simplicity of the model, the complex superconducting behavior has been neglected making it very simple and computationally fast. The magnetic field of the SMES module found with the more sophisticated model is 3.5 T, while the computed inductance is 2 H.

Table 1. Coil parameter optimization.

Parameter	Value
Inner/Outer radius (m)	0.45/0.49
Turns	26
Layers	52
HTS module length (km)	3.9
Magnetic field (T)	3.9
Inductance (H)	2.1

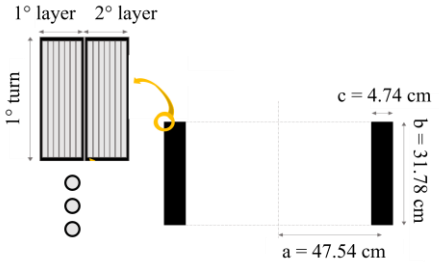

Figure 2. Basic design geometry of the SMES module.

Figure 3 shows the norm of the magnetic flux along the central line and on the top line of the coil, respectively. The maximum magnetic flux density is at the center of the inner part of the coil as expected and its value is lower than the chosen constraint (4 T). Of course, the more sophisticated equations implemented in COMSOL Multiphysics® with respect the one used in the analytical optimization have led to slightly different results. However, a second difference between the two models has been deliberately introduced due to the geometry itself: while the optimization analysis did not care about the electrical insulation, in the computational model the polyimide film thickness is added for evaluating how much the results would have been engraved. Note that despite the maximum magnetic field arises at the center of the coil inner radius, its value on the top (orange circle) is still quite high and is perpendicularly directed towards the coil itself. This means that due to the strong anisotropy of YBCO tapes, the inner top part on the coil would be the most affected in case of unwanted abnormal conditions and that of major interest during transients.

V. Cryostat Design

The cryostat design is intrinsically very complex. It has several functions, among which maintaining the system at cryogenic temperatures, guaranteeing ease access to cryostat components and instrumentation, reducing vibration and ensuring alignment of the equipment therein, guaranteeing the safety and the integrity requirements and ensure the EM screening. Careful considerations must also be done in terms of material properties due to their strongly non-linear temperature dependence [12]. The key role of the present work is to minimize the intrusiveness

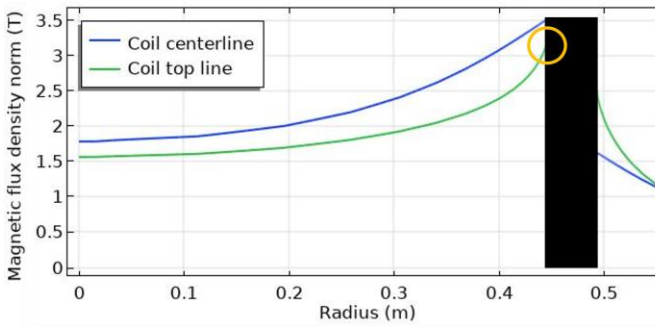

Figure 3. Magnetic flux density computed on two critical lines of the coil.

of the system and to maximize its availability, reliability, and maintainability. In this perspective a dry, cryogen-free, cooling system has been chosen and analyzed, since it is not only less cumbersome to operate and maintain but eliminates the pipes required to circulate the cryogen and its containment structure. It also eliminates the possibility of over-pressurization of the cryostat due to accidental scenarios [13]–[15]. Different cryocooling options have been considered, as well as the thermal behavior of materials, and the thermal stability of the SC magnet.

A. Methodology

An AISI 304 SS vacuum vessel delimits the cryostat from the environment. For reducing the radiation between the cryostat walls, very low emissive materials are used, and an actively cooled radiation shield (Aluminized Kapton film MLI) is added between the high temperature and the low temperature surfaces. A low conductivity thermal shield (Aluminum 6061-T6) is placed between the outermost cryostat wall and the coil to intercept the heat at an intermediate temperature and reduce the conduction heat leak to the lowest temperature.

As result, a two-stages cryogen-free refrigeration can be adopted: the cryostat thermal insulation and the current leads are cooled at the first warmer stage ($\sim 77\ K$) while the magnet itself is cooled at the colder second stage ($\sim 50\ K$). The thermal link between the two-stages and the refrigeration system is provided by two copper plates. This connection between cold heads and thermal loads can also be made 'indirect' using conducting flexible wires to reduce the vibration propagation of the cryocooler through the system.

The basic cryostat design parameters are listed in Table 2, following a similar design as in [13]. A 4 K Gifford-McMahon cryocooler regenerative heat exchanger SRDK-415D is identified to provide the necessary refrigeration power for reaching cryogenic temperatures, with the characteristic and cooling capacity reported in [16]. A preliminary estimation of heat loads due to Joule losses from the current leads, on one hand, and the AC losses during charge/discharge phase, on the other hand, has been performed as follow: for the former, McFee's model of conduction-cooled leads [17] has been applied, giving as result ~45 mW/A at rated temperature; for the latter, the H-formulation [18] has been implemented in COMSOL. The process is based on a 1 s full charge (0 to 1 kA) and a two consecutive 0.5 s charge/discharge phases with a constant current rate of 1.4 kA/s. The result shows that the maximum instantaneous AC loss during the first full charge is ~ 30 W, while that for each charge/discharge phase is ~10 W.

Table 2. Cryostat design parameters.

Component	Parameter	Value
Vacuum Vessel (VV)	Outer radius (m)	0.8
	Thickness (mm)	5
	Height (m)	0.8
Thermal Shield (TS)	Outer radius (m)	0.7
	Thickness (mm)	3
	Height (m)	0.6
Radiation Shield (RS)	Layers	30
	Thickness (mm)	0.9
	Height (m)	0.6

B. Design validation

A 2D axisymmetric geometry is adopted to model the dewar and the coil to solve the conduction equation and compute the required cooling power and the temperature field distribution at the working condition. The heat transfer by radiation is also included as a source term. A preliminary stationary study has been performed fixing the operating temperature at the two cryocooler thermal interfaces (77 K at 1st stage and 50 K at 2nd stage, in absence of any loss but radiation) for also evaluating the number of cryocoolers needed to satisfy the specifications. The results show that, due to the very high cooling capacity of the SRDK-415D at the rated temperature (~25 W at 1st stage and ~30 W at 2nd stage), one single cryocooler would be sufficient to maintain the system at the working temperature. The requested cooling power at the 1st and the 2nd stage are 13.2 W and 0.1 W, respectively. The maximum gradient computed within the winding pack stays below 1 K. However, considering the estimated current leads thermal budget and the peak AC loss, a second cryocooler is necessary to satisfy the specification.

VI. POWER FEEDING SYSTEM

To guarantee the electrical connection to the grid a system of current leads must be foreseen. This is commonly divided in two parts: the ambient temperature current leads, located outside the cryostat, and the cryogenic current leads, located inside the cryostat. The design of the cable at ambient temperature is quite standard, the only requirements are a suitable cross-section to carrying the rated current, without an excessive overheating, and a proper insulation. The section within the cryostat must instead be carefully designed: a normal cryogenic conductor, between the SS chamber and the 1st stage, is commonly used to minimize the cost and to make it properly work (the temperature is still too high for using SC cables); while superconducting current leads (usually made of BSCCO or YBCO tapes) are adopted between the 1st and the 2nd stage to reduce at most the joule losses.

VII. CONCLUSIONS AND PERSPECTIVE

A functional analysis has been applied here for designing a complex SMES system. Throughout this approach all the sub-system and components of a SMES has been broken down and some of them designed in terms of their own independent functions and constraints.

The use of HTS and less complex cryostats allows to design more and more efficient SMES, to be used for the present and crucial energy transition towards a cleaner world. To further assess the soundness of the design, more comprehensive 3D and multi-physics simulations are needed, to fully understand the material behavior (i.e., thermo-mechanics analysis, thermo-magnetic analysis, …). A cryostat optimization should be performed to sustain the maximum heat dissipation during full charge and to reduce the cool down time as much as possible, and finally a multi-elemental toroidal SMES design should be investigated.

REFERENCES

[1] X. D. Xue, K. W. E. Cheng, and D. Sutanto, "A study of the status and future of superconducting magnetic energy storage in power systems," *Supercond. Sci. Technol.*, vol. 19, no. 6, pp. R31–R39, Jun. 2006, doi: 10.1088/0953-2048/19/6/R01.

[2] Mohd. H. Ali, B. Wu, and R. A. Dougal, "An Overview of SMES Applications in Power and Energy Systems," *IEEE Trans. Sustain. Energy*, vol. 1, no. 1, pp. 38–47, Apr. 2010, doi: 10.1109/TSTE.2010.2044901.

[3] M. A. A. Zaman, M. R. Islam, and H. M. A. R. Maruf, "Study on Conceptual Designs of Superconducting Coil for Energy Storage in SMES," *East Eur. J. Phys.*, no. 1, Art. no. 1, Feb. 2020, doi: 10.26565/2312-4334-2020-1-10.

[4] A. Morandi, M. Fabbri, B. Gholizad, F. Grilli, F. Sirois, and V. M. R. Zermeño, "Design and Comparison of a 1-MW/5-s HTS SMES With Toroidal and Solenoidal Geometry," *IEEE Trans. Appl. Supercond.*, vol. 26, no. 4, pp. 1–6, Jun. 2016, doi: 10.1109/TASC.2016.2535271.

[5] A. W. Zimmermann and S. M. Sharkh, "Design of a 1 MJ/100 kW high temperature superconducting magnet for energy storage," *Energy Rep.*, vol. 6, pp. 180–188, May 2020, doi: 10.1016/j.egyr.2020.03.023.

[6] U. Bhunia, J. Akhter, C. Nandi, G. Pal, and S. Saha, "Design of a 4.5MJ/1MW sectored toroidal superconducting energy storage magnet," *Cryogenics*, vol. 63, pp. 186–198, Sep. 2014, doi: 10.1016/j.cryogenics.2014.06.007.

[7] Y. Li, P. Song, Y. Kang, F. Feng, and T. Qu, "Design of a 30-K/4-kJ HTS Magnet Cryocooled With Solid Nitrogen," *IEEE Trans. Appl. Supercond.*, vol. 28, no. 4, pp. 1–6, Jun. 2018, doi: 10.1109/TASC.2018.2814960.

[8] "System Coordination of 2 GJ Class YBCO SMES for Power System Control | Shikimachi, K.; Hirano, N.; Nagaya, S.; Kawashima, H.; Higashikawa, K.; Nakamura, T.

[9] "2G HTS Wire Specification | SuperPower." https://www.superpower-inc.com/specification.aspx (accessed Dec. 10, 2021).

[10] "COMSOL: Multiphysics Software for Optimizing Designs," *COMSOL*. https://www.comsol.com/ (accessed Dec. 10, 2021).

[11] H. B. Brooks, "Design of standards of inductance, and the proposed use of model reactors in the design of air-core and iron-core reactors," *Bur. Stand. J. Res.*, p. 42.

[12] J. G. Weisend II, Ed., *Cryostat Design: Case Studies, Principles and Engineering*. Cham: Springer International Publishing, 2016. doi: 10.1007/978-3-319-31150-0.

[13] Y. S. Choi, D. L. Kim, and D. W. Shin, "Optimal cool-down time of a 4K superconducting magnet cooled by a two-stage cryocooler," *Cryogenics*, vol. 52, no. 1, pp. 13–18, 2012.

[14] H.-M. Chang, Y. S. Choi, and S. W. Van Sciver, "Optimization of operating temperature in cryocooled HTS magnets for compactness and efficiency," *Cryogenics*, vol. 42, no. 12, pp. 787–794, Dec. 2002, doi: 10.1016/S0011-2275(02)00147-9.

[15] Y. Iwasa and K. R. Marken, "*Case Studies in Superconducting Magnets: Design and Operational Issues*," *Phys. Today*, vol. 48, no. 10, pp. 68–68, Oct. 1995, doi: 10.1063/1.2808214.

[16] T. Wirths *et al.*, "Load map of sumitomo 415DP cryocooler in the temperature range of 40-400K," *IOP Conf. Ser. Mater. Sci. Eng.*, vol. 755, p. 012042, Jun. 2020, doi: 10.1088/1757-899X/755/1/012042.

[17] S. Kar *et al.*, "Peformance test and thermal analysis of conduction-cooled optimized current leads at non-optimum operation," Spokane, Washington, USA, 2012, pp. 597–604. doi: 10.1063/1.4706969.

[18] Z. Wang *et al.*, "AC Loss Analysis of a Hybrid HTS Magnet for SMES Based on H-Formulation," *IEEE Trans. Appl. Supercond.*, vol. 27, no. 4, pp. 1–5, Jun. 2017, doi: 10.1109/TASC.2016.2646480.